JOURNAL OF
Materials
CHEMISTRY

Crystal structure and physical properties of (TTM-TTP)AuI_2†

Tadashi Kawamoto,*[a] Masanobu Aragaki,[a] Takehiko Mori,[a] Yohji Misaki[b] and Tokio Yamabe[b]

[a]*Department of Organic and Polymeric Materials, Tokyo Institute of Technology, O-okayama, Tokyo 152, Japan*

[b]*Division of Molecular Engineering, Graduate School of Engineering, Kyoto University, Yoshida, Kyoto 606–01, Japan*

Crystal structure analysis of new organic conductors (TTM-TTP)AuI_2 and (TTM-TTP)$AuBr_2$, where TTM-TTP is 2,5-bis[4,5-bis(methylthio)-1,3-dithiol-2-ylidene]-1,3,4,6-tetrathiapentalene, has been carried out. The donor to anion ratio is 1 : 1 and the donors form highly one-dimensional columns. These materials, however, show dimerization of the donor molecules along the stacking direction. Therefore the energy gap appears at the Fermi level, and these salts become band insulators. The observed temperature dependence of the conductivity is semiconducting, but the room-temperature conductivity is comparatively high, 10–40 S cm^{-1}.

Many bis-fused TTF donors, denoted TTP donors, have been synthesized and many radical-cation salts have been obtained. Most of the radical-cation salts of TTP series donors show metallic behavior down to liquid-He temperature and they are quasi-two-dimensional conductors.[1–3] Among many salts of TTP series donors, only $(DTEDT)_3Au(CN)_2$ shows superconductivity below 4 K at ambient pressure.[4] The radical-cation salts of TTM-TTP (see below), however, are quasi-one-dimensional conductors.[5,6] Although most of the TTM-TTP salts are semiconductors below room temperature, (TTM-TTP)I_3 shows metallic behavior and a metal–insulator transition at 160 K.[6] It is surprising that an organic conductor with a half-filled band, in other words with 1 : 1 composition, shows metallic conductivity, because in general 1 : 1 salts are insulators on account of the on-site Coulomb repulsion. Recently we have observed paramagnetic behavior which is fitted with the one-dimensional Heisenberg model from room temperature to 2 K, without showing any anomaly at the metal–insulator transition temperature. So the low-temperature phase is attributed to the Mott insulator.[7] Such a perfect separation of the spin and charge degrees of freedom has been predicted by the Luttinger liquid theory in the half-filling case. Although the metal–insulator transition temperature is lowered under pressure, the shift is so small that the transition still remains at 90 K even at 11.5 kbar.

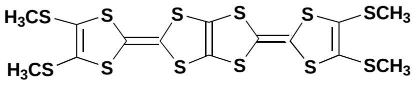

TTM-TTP

In order to apply chemical pressure by the use of shorter anions, preparation of the linear-anion salts other than I_3^- has been attempted. In this paper, crystal structure, energy band structure, and transport properties of (TTM-TTP)AuI_2 and (TTM-TTP)$AuBr_2$ will be shown and discussed in comparison with (TTM-TTP)I_3.

Experimental

TTM-TTP was prepared as described in ref. 8. Crystals of the linear anions were grown by electrochemical oxidation in THF in the presence of the donor and the tetrabutylammonium salts of the corresponding anions under a constant current of 1 μA at 28 °C. These conditions were the same as the case of (TTM-TTP)I_3. In the case of AuI_2^- and $AuBr_2^-$, single crystals were obtained. These crystals were in the form of elongated black thin plates with typical dimensions, 2.0 × 0.14 × 0.08 mm. Their crystal structures were determined by the X-ray single crystal structure analysis.‡

All measurements were made on a Rigaku Raxis II area detector with graphite monochromated Mo-Kα radiation. The structure was solved by the direct method (SHELX86) and was refined by the full-matrix least-squares procedure.[9] Neutral atom scattering factors were taken from ref. 10. Anisotropic thermal parameters were adopted for all non-hydrogen atoms. From the result of the X-ray crystal structure analysis, the electronic structure was calculated on the basis of the extended Hückel method.[11]

Electrical resistivity was measured by the four-probe method using low-frequency ac current (usually 10 μA).

Results

Crystal structures

Crystallographic data are listed in Table 1. The lattice constants show that the AuI_2^- and the $AuBr_2^-$ salts are isostructual. Although the structure analyses were carried out for both salts, the data of the $AuBr_2^-$ salt are not very good owing to its poor crystal quality. Then we will concentrate on the results of the AuI_2^- salt.

The atomic numbering scheme is shown in Fig. 1(*a*). The length of the *c* axis of the AuI_2^- salt is almost twice as long as that of the I_3^- salt, indicating that the donor molecules form a dimer along the stacking direction. The I_3^- salt has only one donor molecule in a unit cell, but one unit cell contains two donor molecules in the present compounds. In (TTM-TTP)I_3 the donor molecule is located on an inversion

---

* kawamoto@o.cc.titech.ac.jp

† Presented at the 58th Okazaki Conference, Recent Development and Future Prospects of Molecular Based Conductors, Okazaki, Japan, 7–9 March 1997.

‡ Full crystallographic details, excluding structure factors, have been deposited at the Cambridge Crystallographic Data Centre (CCDC). See Information for Authors, *J. Mater. Chem.*, 1996, Issue 1. Any request to the CCDC for this material should quote the full literature citation and the reference number 1145/56.

Table 1 Crystallographic data

	(TTM-TTP)AuI_2	(TTM-TTP)$AuBr_2$
chemical formula	$C_{14}H_{12}S_{12}AuI_2$	$C_{14}H_{12}S_{12}AuBr_2$
formula weight	1015.876	921.876
shape	black plate	black plate
crystal system	triclinic	triclinic
space group	$P\bar{1}$	$P\bar{1}$
a/Å	12.745(6)	12.49(5)
b/Å	13.641(6)	13.39(4)
c/Å	9.410(8)	9.41(4)
α/°	107.39(6)	107.3(3)
β/°	104.54(8)	104.2(4)
γ/°	100.08(4)	100.2(2)
V/Å^3	1454(2)	1402(12)
Z	2	2
D_c/g cm^{-3}	2.320	2.184
λ/Å	0.71070	0.71070
temperature/K	298	298
μ(Mo-Kα)/cm^{-1}	79.86	89.24
R	0.071	0.100
$R_w{}^a$	0.097	0.119
reflections used	2237	1256

$^a w = 1/\sigma(I)^2$.

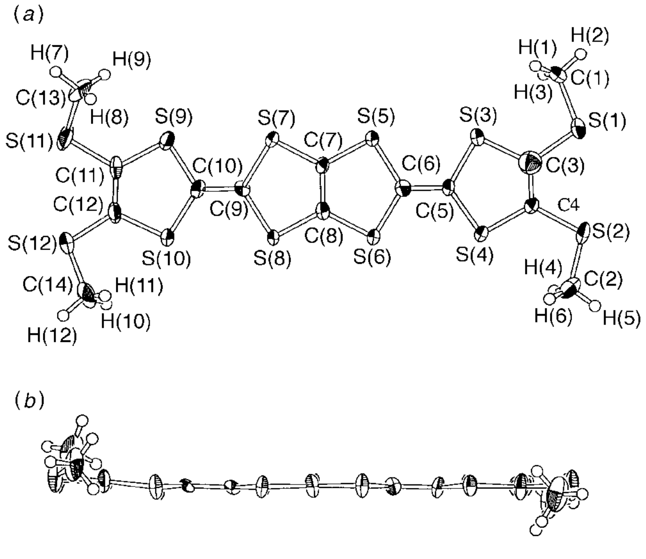

Fig. 1 (*a*) ORTEP drawing and atomic numbering scheme of the donor molecule of (TTM-TTP)AuI_2 and (*b*) side view of the molecule of (TTM-TTP)AuI_2

center.[6] In the $AuI_2{}^-$ salt, however, the donor molecule is located on a general position. A unit cell contains two $AuI_2{}^-$ anions on general equivalent positions [Fig. 2(*a*)]. In (TTM-TTP)I_3 there are short I···I contacts of 4.235(1) Å, while in the present compound the closest I···I distances are 4.566(6) and 5.102(4) Å. Since these values are larger than the van der Waals distance of I^-, 4.2 Å, we can regard the anions as discrete $AuI_2{}^-$. No anion deficiency was found from the structure analysis; therefore this complex has exact 1:1 composition.

The donor molecule is almost planar; the deviations from the least-squares plane are less than 0.2 Å except for the terminal methylthio groups [Fig. 1(*b*)]. The terminal C—S bonds also extend basically in the molecular plane except for C(13); the deviation of C(13) from the least-squares plane is 1.16 Å. In the present donor, the terminal carbons of the neutral molecule are reported to be out of the molecular plane.[8] In contrast, in (TTM-TTP)I_3 with +1 charge the molecular structure is flat.[6] Therefore the flat molecular structure of the present salt is consistent with the expected +1 charge.

Intramolecular bond lengths (averaged so as to have hypothetical *mmm* symmetry) are listed in Table 2. Although the changes of the bond lengths, when the donor is oxidized from neutral to +1, are comparable to the estimated standard deviations of the bond lengths, particularly in such cases as the present compound that contains heavy atoms like Au and I, comparing the bond lengths after averaging under the *mmm* symmetry, we can make an approximate estimate of the degree of charge transfer, as exemplified in ref. 13. In comparison with the neutral TTM-TTP, most C=C bonds become longer, and most C—S bonds become shorter. This is consistent with the symmetry of the HOMO, which has nodes on all C—S bonds. The bond lengths in (TTM-TTP)AuI_2 are very close to those in (TTM-TTP)I_3. This also demonstrates that the donor molecule of this salt has +1 charge. The differences of the bond lengths between D^0 and D^+ are, however, as small as 0.01–0.03 Å; these values are about half of the corresponding changes in the TTF series, 0.02–0.07 Å.[12] This is reasonable because the HOMO of the TTM-TTP molecule spreads on the larger molecule as pointed out in ref. 6.

The donor molecules are stacked along the *c* axis [Fig. 2(*b*)]. Fig. 3 shows the overlap modes in the stack. Because the donor molecules dimerize along the stacking direction, there are two overlap modes. Both modes are ring-over-bond type. In one overlap mode denoted c1 in this stack [Fig. 2(*b*) and Fig. 3(*a*)], the slip distance along the molecular long axis is 1.6 Å, which corresponds to about half of the length of a 1,3-dithiole ring. The interplanar distance of the c1 mode is 3.46 Å, where the plane of the donor molecule is defined by the bis-fused TTF part, but the CH_3S parts are excluded. The other overlap mode denoted c2 [Fig. 2(*b*) and Fig. 3(*b*)] is the same as the uniform overlapping mode in (TTM-TTP)I_3; the slip along the molecular long direction of c2 is 4.8 Å, which corresponds to one and a half 1,3-dithiole rings. The interplanar distance of c2 is 3.48 Å. This is slightly larger than that of the c1 mode. These stacking overlap modes have many S—S contacts shorter than the van der Waals distance.

Energy band structures

Calculated intermolecular overlap integrals of the HOMO are listed in Table 3. The difference between c1 and c2 designates the degree of dimerization along the stack. The ratio of c1 to c2 is about 3:2, therefore the dimerization is not so strong. The intrastack overlaps are 200 times as large as those of interstack overlaps. Along [1$\bar{1}$0], the donor molecules cannot approach close to each other because of the steric hindrance of the terminal methyl groups. So the side-by-side interaction along the molecular short axis is very small. This situation has a close resemblance to (TTM-TTP)I_3. Therefore the electronic

Table 2 Intramolecular bond lengths (Å) of TTM-TTP averaged by assuming *mmm* symmetry

salt	C(7)—C(8)	S(5)—C(7) S(6)—C(8) S(7)—C(7) S(8)—C(8)	S(5)—C(6) S(6)—C(6) S(7)—C(9) S(8)—C(9)	C(5)—C(6) C(9)—C(10)	S(3)—C(5) S(4)—C(5) S(9)—C(10) S(10)—C(10)	S(3)–C(3) S(4)—C(4) S(9)—C(11) S(10)—C(12)	C(3)—C(4) C(11)—C(12)
neutral	1.346(7)	1.743(4)	1.764(4)	1.348(6)	1.752(4)	1.754(4)	1.339(4)
I_3	1.362(9)	1.732(9)	1.748(6)	1.38(1)	1.737(8)	1.752(8)	1.351(9)
AuI_2	1.37(4)	1.73(3)	1.76(3)	1.38(3)	1.74(3)	1.75(3)	1.33(4)

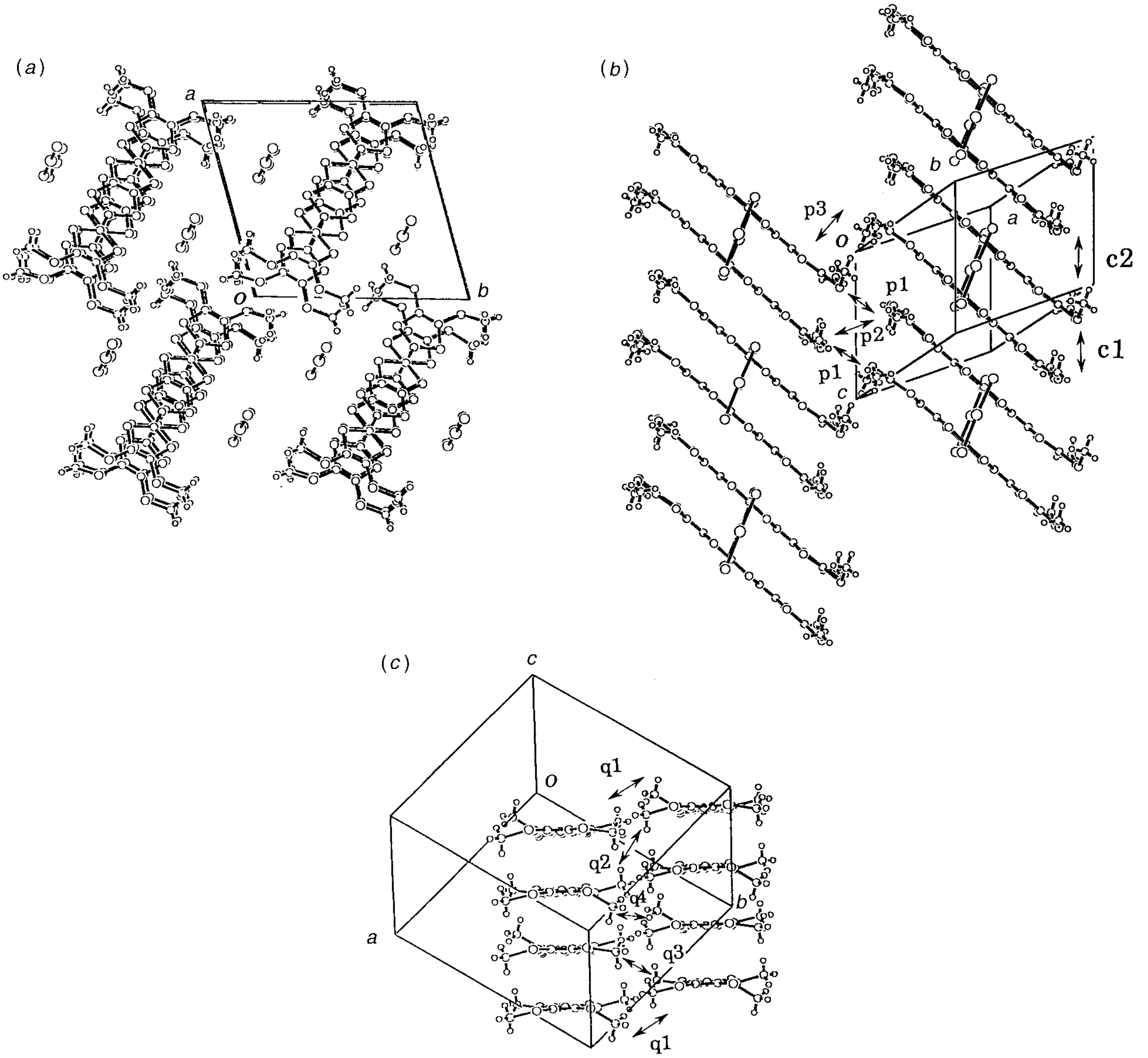

Fig. 2 Crystal structure of (TTM-TTP)AuI_2. (*a*) Projection onto the *ab* plane, (*b*) view along the molecular short axis, and (*c*) view along the molecular long axis.

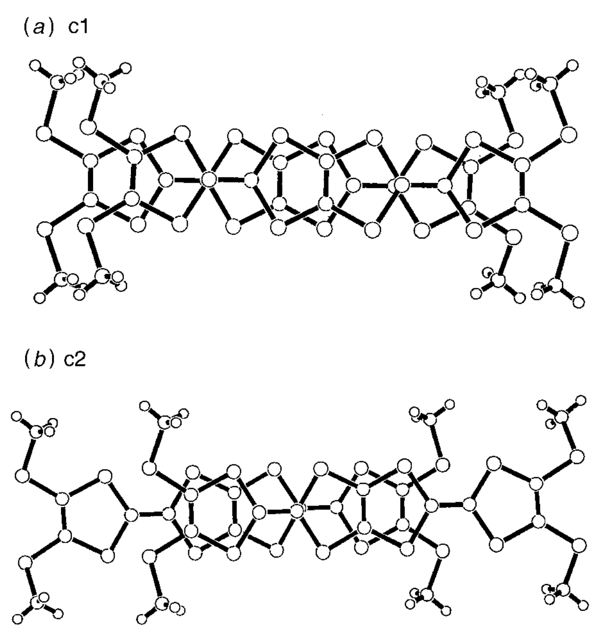

Fig. 3 Overlap modes of intrastack interactions in (TTM-TTP)AuI_2

Table 3 Intermolecular overlap integrals, S ($\times 10^3$) of the HOMO of (TTM-TTP)AuI_2

c1	27.4	c2	19.1	p1	−0.07
p2	−0.01	p3	0.19	q1	−0.17
q2	−0.03	q3	−0.10	q4	−0.05

structures of the present materials are regarded as highly one-dimensional.

Fig. 4 shows the energy band structure calculated on the basis of the extended Hückel orbital calculation and the tight-binding method. Because a unit cell contains two donor molecules, there are two energy bands. This is different from (TTM-TTP)I_3. As a result of the 1:1 composition, the band is half-filled like the I_3^- salt. The energy gap, however, exists at the Fermi level, and thus no Fermi surface exists. This band structure predicts that the present salts are band insulators.

Transport properties

The conductivity at room temperature is about 10 and 40 S cm^{-1} for the AuI_2^- and $AuBr_2^-$ salts, respectively. These conductivities are much lower than that of (TTM-TTP)I_3.[6] These values are, however, comparatively high for a band insulator with a dimerized structure. Fig. 5 shows the tempera-

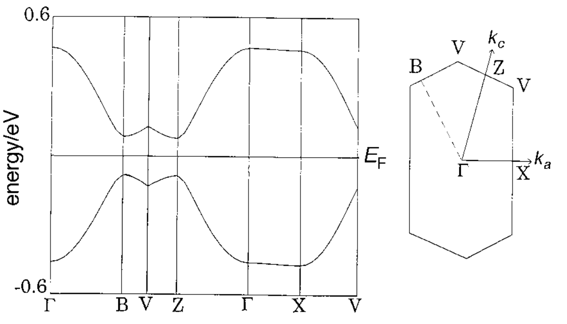

Fig. 4 Tight-binding energy band structure of (TTM-TTP)AuI_2 calculated from the overlap of the HOMO obtained on the basis of the extended Hückel molecular orbital calculation

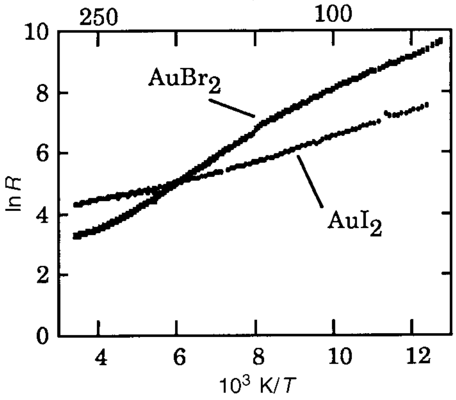

Fig. 5 Temperature dependence of electrical resistance of (TTM-TTP)AuI_2 and (TTM-TTP)$AuBr_2$

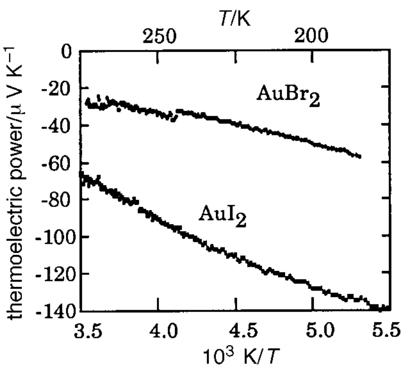

Fig. 6 Temperature dependence of thermoelectric power of (TTM-TTP)AuI_2 and (TTM-TTP)$AuBr_2$

ture dependence of electrical resistance of (TTM-TTP)AuI_2 and (TTM-TTP)$AuBr_2$ at ambient pressure. These salts were semiconductors below room temperature. From the inclinations of the straight lines in this figure, the activation energies are extracted to be 0.03 eV for the AuI_2^- salt, and 0.07 eV for the $AuBr_2^-$ salt. This semiconducting behavior is in agreement with the energy band calculation.

Thermoelectric power (Seebeck coefficient) of the AuI_2^- and $AuBr_2^-$ salts were measured as shown in Fig. 6. The sign of the thermopower is negative in both salts. This means that the mobility of electrons is higher than that of holes. The value of $|Q|$ is proportional to $1/T$ as the temperature decreases, as expected in a semiconductor.[13] From Fig. 6 activation energies are estimated to be 0.08 eV for the AuI_2^- salt, and 0.05 eV for the $AuBr_2^-$ salt.

Discussion

The AuI_2^- and $AuBr_2^-$ salts of TTM-TTP were obtained by the electrochemical crystal growth method similarly to (TTM-TTP)I_3. These salts have the same 1 : 1 composition as the I_3^- salt. These salts, however, have the dimerization of the donor molecules along the stacking direction. Therefore the energy gap appears at the Fermi level, and these salts become insulators. The observed conducting behaviors agree with this expectation from the crystal structure.

The application of chemical pressure, namely the use of shorter anions, induces dimerization. In contrast, a naive prediction suggests that a uniform structure is generally more preferable under pressure, as most Peierls transitions are suppressed under pressure. Although the AuI_2^- anion (9.4 Å) is shorter than the I_3^- anion (10.1 Å),[14] the lattice volume of the AuI_2^- salt is larger than twice that of the I_3^- salt. On the other hand the lattice constant *c* of the AuI_2^- salt is significantly shorter than twice that of the I_3^- salt. In these salts the linear anions are placed almost parallel to the intermolecular vector between the centers of dimerized molecules, and so are slightly inclined from the stacking direction. Therefore it is considered that the shrinkage of the linear anion makes crystal packing with a uniform stacking similar to the I_3^- salt impossible, and gives rise to the change of the stacking pattern, resulting in the dimerization. As a result the AuI_2^- salt becomes a band insulator. The lattice volume, however, increases owing to the change of the stacking pattern. Thus we cannot use shorter anions as a source of chemical pressure in the present case.

The dimerization of the present compounds can be regarded as 'chemically induced' Peierls instability. One of the greatest mysteries in (TTM-TTP)I_3 is the absence of the Peierls transition. Here we have encountered such an instability entirely unexpectedly.

References

1 Y. Misaki, H. Fujiwara, T. Yamabe, T. Mori, H. Mori and S. Tanaka, *Chem. Lett.*, 1994, 1653.

2 T. Mori, Y. Misaki, H. Fujiwara and T. Yamabe, *Bull. Chem. Soc. Jpn.*, 1994, **67**, 2685.

3 T. Mori, T. Kawamoto, Y. Misaki, K. Kawakami, H. Fujiwara, T. Yamabe, H. Mori and S. Tanaka, *Mol. Cryst. Liq. Cryst.*, 1996, **284**, 271.

4 Y. Misaki, N. Higuchi, H. Fujiwara, T. Yamabe, T. Mori, H. Mori and S. Tanaka, *Angew. Chem., Int. Ed. Engl.*, 1995, **34**, 1222.

5 Y. Misaki, H. Nishikawa, T. Yamabe, T. Mori, H. Mori and S. Tanaka, *Synth. Met.*, 1995, **70**, 1153.

6 T. Mori, H. Inokuchi, Y. Misaki, T. Yamabe, H. Mori and S. Tanaka, *Bull. Chem. Soc. Jpn.*, 1994, **67**, 661.

7 T. Mori, T. Kawamoto, J. Yamaura, T. Enoki, Y. Misaki, T. Yamabe, H. Mori and S. Tanaka, *Phys. Rev. Lett.*, 1997, **79**, 1702.

8 Y. Misaki, H. Nishikawa, K. Kawakami, S. Koyanagi, T. Yamabe and M. Shiro, *Chem. Lett.*, 1992, 2321.

9 G. M. Sheldrick, *Crystallographic Computing 3*, Oxford University Press, Oxford, 1985, pp. 175–189.

10 D. T. Cromer and J. T. Waber, *International Tables for X-Ray Crystallography*, Kynoch Press, Birmingham, 1974, vol. 4, Table 2.2 A.

11 T. Mori, A. Kobayashi, Y. Sasaki, H. Kobayashi, G. Saito and H. Inokuchi, *Bull. Chem. Soc. Jpn.*, 1984, **57**, 627.

12 H. Kobayashi, R. Kato, T. Mori, A. Kobayashi, Y. Sasaki, G. Saito, T. Enoki and H. Inokuchi, *Mol. Cryst. Liq. Cryst.*, 1984, **107**, 33.

13 P. M. Chaikin, R. L. Greene, S. Etemad and E. Engler, *Phys. Rev. B.*, 1976, **13**, 1627.

14 J. M. Williams, J. R. Ferraro, R. J. Thorn, K. D. Carlson, U. Geiser, H. H. Wang, A. M. Kini and M.-H. Whangbo, *Organic Superconductors (Including Fullerenes): Synthesis, Structure, Properties, and Theory*, Prentice Hall, NJ, 1992.

Paper 7/03200E; *Received* 9*th May*, 1997